Faraday Discussions

Cite this: *Faraday Discuss.*, 2014, **171**, 429

PAPER

Approaches to time-resolved diffraction using an XFEL

John C. H. Spence*

Received 27th February 2014, Accepted 25th March 2014
DOI: 10.1039/c4fd00025k

We describe several schemes for time-resolved imaging of molecular motion using a free-electron laser (XFEL), in response to the many challenges and opportunities which XFEL radiation has created for accurate time-resolved measurement of structure. For pump–probe experiments using crystals, the problem of recording full Bragg reflections (not partials) in each shot arises. Two solutions, the use of the large bandwith which necesarily results from using attosecond pulses, and the use the coherent convergent beam mode are suggested. We also show that with attosecond recording times shorter than the temporal coherence time, Bragg reflections excited by different wavelengths from different reflections can interfere, providing structure factor phase information. For slower processes, a mixing jet sample-delivery device is described to allow snapshot solution scattering during molecular reactions on the microsecond scale. For optically excited membrane proteins, we suggest the use of the lipid cubic phase sample delivery device operating at atmospheric pressure. The use of two-color and split-and-delay schemes is suggested for improved accuracy in the Monte-Carlo method of serial femtosecond crystallography (SFX).

1. Introduction

Understanding of the function of biological macromolecules requires mapping of their three-dimensional (3D) structures at near-atomic resolution, together with observation of the dynamics of these structures during a chemical reaction or optical excitation. This has previously been achieved using "pump–probe" experiments based on time-resolved (TR) crystallography in the Laue mode,[1] over timescales from picoseconds to seconds.[2] Issues of reaction branching, the fraction of excited molecules in the crystal, and the periodic averaging over unit cells in the reconstructed density map are discussed elsewhere.[2] The conventional method of protein crystallography (MX), in which a sample is rotated slowly through the Bragg condition to provide angle-integrated reflections, cannot be used if a series of snapshots showing the molecular motions is required. (An angle integration over the crystal rocking curve is needed to obtain a structure factor). In the Laue method, fast integrated reflections are obtained by using broad-band

Department of Physics, Arizona State University, Tempe, Az., USA 85282

radiation in the transmission geometry, so that the corresponding range of Ewald sphere diameters spans the rocking curves of reflections near the Bragg condition, while also generating more reflections per exposure. This range of diameters is shown as the area AOB in Fig. 1.

Time-resolved measurements require a fast trigger to initiate the reaction in the crystal, followed after a delay by the recording of a diffraction pattern from the excited state of the crystal. Difference density maps are formed between the ground and excited states, with a different delay for each frame of a "movie". Many crystal orientations are needed for each delay for a 3D image reconstruction. Full, rather than partial, Bragg reflections must be recorded in each snapshot, which is then probed at different time points along the reaction coordinate, until complete data sets are obtained.

The invention of the hard X-ray laser[3] with its femtosecond pulses of intense radiation has created both opportunities and challenges for TR-MX. The first hard-X-ray XFEL, the Linac Coherent Light Source (LCLS) at SLAC, for example, provides about 1E12 photons of 8 kV radiation per pulse at 120 Hz repetition rate, into a focused spot as small as 0.1 micron diameter. Since the focused beam instantly vaporizes the sample and the shot-to-shot variations in beam intensity are large (eg 15%), while the beam is relatively monochromatic (eg 0.1% energy spread), Laue diffraction for TR-MX by the conventional method is impossible. However it has been found that these femotosecond pulses outrun radiation damage[4] so that atomic-resolution diffraction patterns are detected before the onset of serious damage from impact ionization due to the photoelectron cascade. (The limited direct ionization effects which occur during the pulse are unimportant for most MX applications, and detection ends well before the onset of atomic motion). The resulting need to maintain a fresh supply of protein nanocrystals for this "diffract-then-destroy" mode has been satisfied by using a

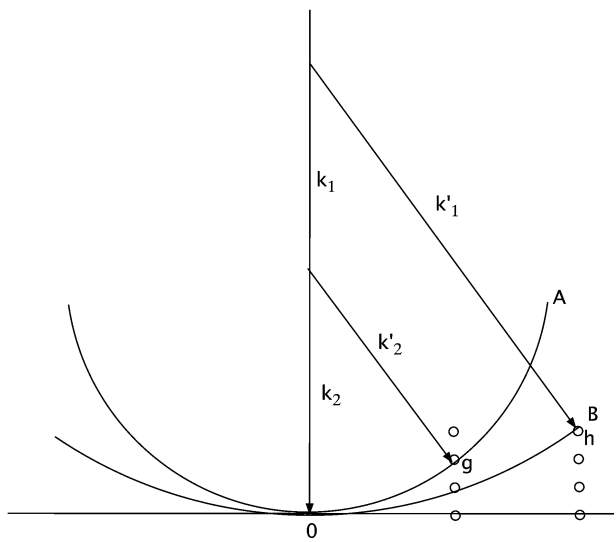

Fig. 1 Ewald sphere scattering geometry for two wavelengths scattering from different reflections into the same detector pixel. With a bandwidth spanning wavevectors from $\mathbf{k}_1$ to $\mathbf{k}_2$, all Bragg reflections falling within the area AOB are excited.

liquid jet a few microns in diameter, running across the pulsed X-ray beam in vacuum, carrying the appropriate concentration of protein nanocrystals. This has led to the development of the serial femtosecond crystallography (SFX) method (see[5] for a review). The first pump–probe experiments using a liquid jet for time-resolved SFX have recently been reported, applied to a stream of optically excited Photosystem 1 - ferredoxin nanocrystals, important for photosynthesis.[6] These showed changes in structure factors due to illumination which well exceeded the noise level. In this method, a pump laser crosses the liquid jet immediately prior to their transit of the X-ray beam. Diffraction patterns from excited and ground-state nanocrystals are interleaved, however normalization is difficult, since each crystal is a different size and each snapshot provides only partial reflections. One relies on the chance occurrence among millions of patterns to provide a range of orientations across the rocking curve (from nanocrystals of different size).

While this pump–probe-in-a-jet approach holds promise, the Monte Carlo process used to merge data (which averages over all stochastic experimental variables, such as beam intensity variations, nanocrystal size and orientation) converges slowly as 1/sqrt(N) for N shots, and is very wasteful of protein, since all protein between shots runs to waste. In addition, the time-resolution of the EXFEL is far better than needed for biological studies, where molecular motions occur on a time-scale of microseconds to milliseconds. Nevertheless we wish to take advantage of the absence of radiation damage made possible by the use of femosecond snapshots with destructive readout. In this paper we review some alternative schemes for TR-SFX under development. Among many challenges when attempting to use the poorly characterized experimental conditions of an XFEL for the highly accurate quantification of data needed in time-resolved work, we focus here mainly on the problem of obtaining full, rather than partial, Bragg reflections.

2. Attosecond Laue diffraction

A proposal has recently been made to construct an attosecond (as) hard-X-ray laser, based on a coherent inverse Compton scattering (C-ICS) source.[7] This machine is currently under construction at DESY in Germany, and is much smaller than an XFEL. Taking pulses to be bandlimited and to have full temporal coherence, the pulse duration Δt and beam energy spread ΔE are then related by the uncertainty principle as

$$\Delta t\ (\text{fs}) = 4.14/\Delta E\ (\text{eV}) \tag{1}$$

the necessary energy spread for Laue diffraction of, say, 3% at 10 kV can then be obtained using 14 as pulses, giving a bandwidth of 300 eV. These pulses will certainly also outrun radiation damage. The crystalline sample then acts as a monochromator, picking out wavelengths which satisfy Bragg's law for many reflections, and spanning their rocking curves.[1] In this way both radiation damage avoidance and Laue snapshot diffraction with full reflections becomes possible when using sufficiently brief pulses.

For bandlimited pulses, two different reflections may scatter at different wavelengths λ_1 and λ_2 into the same direction $\mathbf{k}_1$ (or $\mathbf{k}_2$) and detector pixel, as shown in Fig. 1. These will interfere coherently if the pulse duration is sufficiently

brief. Then the resulting intensity will contain information on structure factor phase. Interference occurs if the recording time τ (the pulse duration) is less than the beat period T between the frequencies of the two wavelengths $\omega_1 = \mathrm{c}\,\mathrm{k}_1 = 2\pi\, c/\lambda_1$ and $\omega_2 = c\,k_2 = 2\pi\, c/\lambda_2$, satisfying the two different Bragg conditions, and this will be so if the pulses are bandlimited. For a crystal wider than the focused beam and thicker than an extinction distance, aside from unimportant constants, the scattered intensity in a single pulse in direction $\mathbf{k}_2'$ is

$$I_T = \int_0^\tau \left| F(g)\exp\left(ik_1'\cdot r + i\varpi_1 t\right) + F(h)\exp\left(ik_2'\cdot r + i\varpi_2 t\right)\right|^2 \mathrm{d}t \qquad (2)$$

If the recording time $\tau < T = 2\pi/(\omega_1 - \omega_2)$ and the complex structure factors are $F(\mathbf{g}) = f(\mathbf{g})\ \exp\ (i\ \theta_\mathbf{g})$, this becomes

$$I_T = f(g)^2 + f(h)^2 + 2|f(g)||f(h)|\cos\left(\theta_g - \theta_h\right) \qquad (3)$$

which is sensitive to the phase difference between structure factors F_g and F_h. The result depends on choice of origin for **r**. Phase sums which are independent of origin can be formed if the corresponding reciprocal lattice vectors sum to zero (forming a closed loop in reciprocal space), and may be found in this case if absorption is neglected and Freidel symmetry assumed. Then such loops can be formed within the region AOB of Fig. 1.

3. Coherent convergent-beam diffraction

A second method for obtaining full reflections in a single shot is provided by convergent-beam diffraction. The geometry is shown in Fig. 2. We see that since

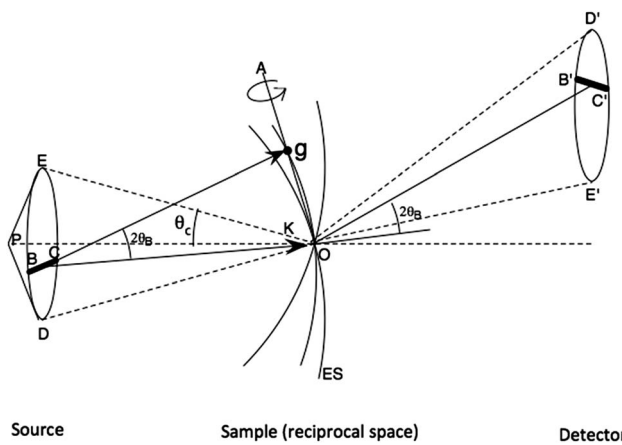

Fig. 2 Coherent convergent-beam diffraction geometry, showing source DE, Ewald sphere ES and detector E′D′. Point source P fills illumination aperture DE coherently. Limiting Ewald sphere orientations (eg ES) are defined by marginal rays DO and EO. Plane-wave component K of converging spherical wave (with beam divergence θ_χ) from midpoint of BC arrives at detector at midpoint of B′C′. Rotation of arrowed wavevectors originating along line BC about OA preserves the Bragg condition for reciprocal lattice vector **g**, defining line C′B′ at detector, along which the Bragg condition is satisfied, producing Bragg lines instead of spots. The disk E′D′ is an inverted image of ED.

the Bragg condition for reflection **g** is preserved when a crystal is rotated about **g**, it follows that for a stationary crystal, wavevectors within the illumination cone of semiangle θ_χ which rotate about **g** also preserve this condition, producing a line of intensity at the detector instead of a Bragg spot. The intensity profile across this line is then the crystal rocking curve, which may be measured, given sufficiently fine pixelation. In this way, the covergent beam method provides an "angular window" across the crystal rocking curve in each reflection simultaneously which lies near a Bragg condition. Integration across the line of intensity then gives full reflections, proportional to structure factors, as required for "single-shot" Laue diffraction.

If the illumination is coherent, as from an XFEL, an extremely small beam diameter can be produced, of diffraction-limited diameter $d_p \sim 1.2\ \lambda/\theta_\chi$ between first minima. Such small beams become smaller than one mosaic block, so that that the traditional theory of mosaicity with its smooth modelled rocking curve does not apply, and the shape transforms seen in experimental XFEL data must be considered when merging data.[13] By combining this expression for d_p (which ignores aberrations in the probe-forming optics) with Bragg's law $\lambda = 2\ d_{hkl} \sin(\Theta_B)$, putting $d_{hkl} = d_p/2$, we see that when the beam radius is just equal to the unit-cell dimension (for a first-order reflection) then the coherent convergent-beam disks will overlap and interfere by about 22%. (The current LCLS micro-diffraction beam diameter of 100 nm is not much bigger than the unit cell of some macromolecular crystals or viruses). This interference between coherent overlapping orders provides information on structure factor phases (reckoned about an origin at the center of the beam).[8] It has been demonstrated both in electron[8] and soft X-ray diffraction.[14] For protein crystallography, where autoindexing of a large number of reflections in three-dimensions is required, the requirement on beam divergence is that it be somewhat less than the Bragg angle, in order that individual reflections can be indexed without overlap in three dimensions on the curved Ewald sphere. Using simulations, we have shown the more rapid convergence of SFX data which results when beam divergence increases. Here the standard deviation R_{split} in the sum of the same reflection from N different nanocrystals of different size in slightly different orientations is plotted against the number of nanocrystals, and the results found to fall more rapidly as N increases due to the decrease in "partiality" which results from larger beam divergence. This experimental requirement for larger beam divergence of a few milliradians is entirely practical for protein crystals.

4. Mixing jets

The liquid injector system used to spray submicron nanocrystals across the XFEL beam in a liquid stream a few microns in diameter, flowing in vacuum at about 10 m s^{-1} has been described in several papers.[9] The stream is surrounded by a coaxial jacket of high-pressure gas, which, by speeding up the liquid, focuses the stream. In this way, clogging is avoided by allowing the use of a larger nozzle but much finer focused liquid stream, which breaks up by Rayleigh instability into a stream of micron-sized droplets.

The arrangement consists of a hollow fiber-optic line (carrying the buffer and nanocrystal solution) running inside a glass capillary tube, with high pressure helium gas between the two tubes, emerging at the nozzle to focus the liquid.

A new version has now been made for the study of time-resolved chemical reactions in solution at an EXFEL.[10] As shown in Fig. 3, a third tube is used between the inner fiber and outer capillary. The space between this tube and the fiber supplies a second liquid, while gas outside it (and within the capillary tube) provides the focusing effect. The inner hollow fiber-optic tube slides telescopically along inside the intermediate tube to vary the reaction time of two fluids. In a typical experiment, a substrate may be supplied in the intermediate space, and an enzyme in solution in the fiber-optic line along the axis. With the fiber withdrawn, the two fluids, catalyst and substrate, mix at the end of the fiber, then react as they travel to the nozzle leading into vacuum. EXFEL shots then provide snap-shot SAXS data for different reaction times as the inner fiber is slowly withdrawn. The theory of these fluctuation SAXS patterns (FSAXS), originally given by Z. Kam, in which the recording time is much shorter than the rotational diffusion times of the molecules, has been reviewed elsewhere.[11] In particular, the patterns are two-dimensional, unlike conventional isotropic one-dimensional SAXS patterns, and hence contain more information to assist a three-dimensional reconstruction. (Two-dimensional scattering due to coherent interference between X-rays scattered from different particles is not used.) Experiments with this new mixing jet are planned for the near future and the performance of the jet has been evaluated using fluorescent dyes. The range of reaction times possible is 10–200 milliseconds, appropriate to many biological systems, while the mixing time at the end of the inner fiber, before reactions begin, is about 200 microseconds, and this sets the error in reaction timing measurement for each movie frame. In this way we hope to track the molecular motions involved in enzyme catalysis.

5. Pump–probe LCP jet experiments

In order to eliminate the protein which flows to waste between XFEL shots (at 120 Hz), a new sample injector has been developed using a more viscous medium, lipidic cubic phase (LCP).[12] Only about 1 out of 10,000 nanocrystals produce X-ray patterns in the earlier liquid jet, running at 10 m s^{-1} with a flow rate 10 microliters/min, requiring perhaps 10–100 mg of pure protein for 5 h of data collection.

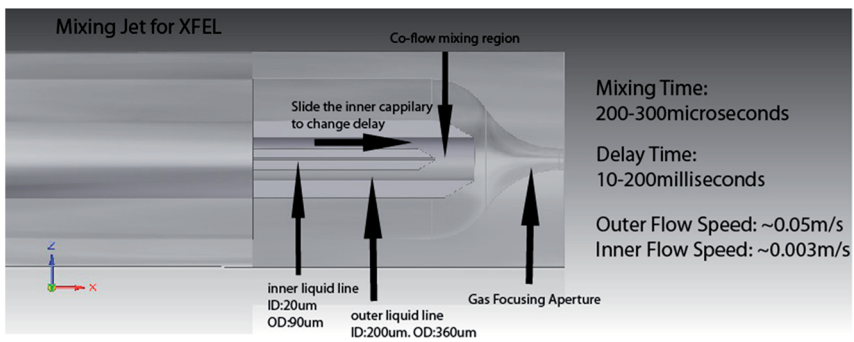

Fig. 3 Mixing jet, showing three concentric tubes and nozzle. Two fluids are mixed in a short mixing time, then allowed to react for a delay time before emerging from the nozzle in a jet a few microns in diameter. This is intercepted by the pulsed X-ray beam. By sliding the inner tube, the delay time can be adjusted.

The slower, more viscous LCP jet, with flow rate between 1–300 nl min^{-1}, then greatly reduces wasted protein by a factor of about 20, and also provides both a growth medium (for both membrane and some soluble proteins) in which to grow nanocrystals, while at the same time running slowly enough to produce a high hit rate (the nanoxtals emerge from this "toothpaste jet" at about the same rate as the X-ray pulses arrive). The jet has proven particulary useful for study of the important GPCR class of proteins, which may form nanocrystals but do not grow large enough crystals for conventional protein crystallography (MX). Fig. 4 shows recent results for XFEL diffraction from human serotonin receptor[12] and an image of the LCP jet running. Using photosensitive membrane proteins in this sample delivery system, it should also be possible to undertake pump–probe experiments for the microsecond time-scales (and longer) involved in biology. Experiments are planned to determine the maximum repetition rate of the XFEL which allows debris to be cleared due to the vaporization of one sample, before the next moves into place on the X-ray optic axis. The possibility is also being explored of doing this work at atmospheric pressure (or in a helium environment), since the LCP jet is found to work satisfactorily in air at STP.

6. Other approaches, discussion

For the TR-SFX experiments undertaken to date,[6] the Monte Carlo method of data analysis has been used.[13] This means that X-ray snapshots for the ground and excited state in a pump–probe experiment are taken from different nanocrystals of different size (each of which is destroyed after recording these patterns). In addition, one has shot-to-shot intensity variations of perhaps 15% when using an XFEL, much larger than the effect on structure factors of the pump laser. While scaling methods have been developed to deal with this, greater accuracy could be

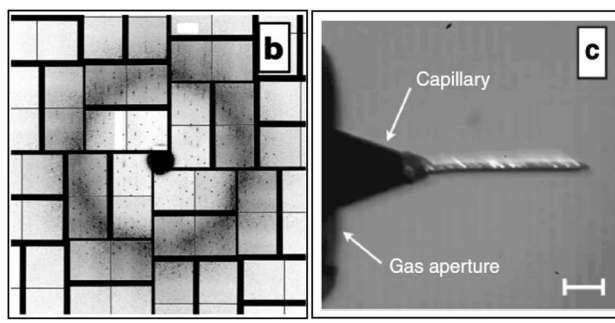

Fig. 4 (b) Diffraction from serotonin receptor 5-HT_{2B} in cholesterol-doped 9.9 MAG + 7.9 MAG LCP. No sharp rings are visible suggesting that formation of L_c phase has been avoided (X-ray intensity attenuated to 3.1% due to strong Bragg diffraction from 5 × 5 × 5 μm^3 sized crystals, 1.5 μm X-ray beam diameter, 50 fs pulse length, 9.5 keV, 50 μm LCP jet diameter, 190 nL min^{-1} flow rate, 120 Hz pulse rate). The resolution at the detector edge in both panels is 2.5 Å.[12] c) 9.9 MAG LCP extrusion in vacuum viewed between crossed polarizers. The tapered end of the capillary nozzle is seen protruding out of the gas aperture. Capillary inner diameter: 30 μm. With He as co-flowing gas. Birefringence (bright flecks) is an indication of a transition of the cubic phase to a lamellar crystalline phase due to evaporative cooling.

obtained if two snapshots, for ground and excited state, could be obtained from the same crystal. In this case the first shot must be below the damage threshold for the protein nanocrystal. These experimental conditions will become available with the development of "two-color" experiments, in which, using seeded beams or two undulators and gain modulation, it is possible to produce a pair of X-ray pulses of slightly different wavelength, with a delay between them. At present these delays are limited to a few hundred femtoseconds. Between these pulses must be inserted the pump laser pulse. It is not possible to read out two diffraction patterns separated by such a brief time interval, however their different wavelengths will displace them slightly on the detector, so that they may be read out together as a single frame. A serious challenge with this arrangement is the reduction of timing jitter on the pump laser, which must be less than the time between pulses.

Alternatively, schemes have been developed for "split-and-delay" of the X-ray pulses, using either mirrors or Bragg beam splitters. The beam is split into two beams of equal intensity, and one pulse sent on a longer optical path to introduce delay (the speed of light is 3.3 ns m^{-1}, so that a very long detour is needed to obtain the microsecond delays important for biology). Timing jitter on the pump laser is no longer an issue, but the overlap of the two beams in space then becomes challenging if submicron beam diameters are involved. The two beams have the same energy. One may then arrange for the two beams to strike the same nanocrystal (perhaps in LCP) at slightly different angles, so that the immediate and delayed diffraction patterns are displaced again on the detector, for common readout. Since only differences between the intensities of scattering from the same crystals are accumulated, this method can be shown to eliminate most error due to variations in crystal size, orientation and shot-to-shot beam intensity variation. The weaker pulses needed to avoid damage to the crystals do increase noise in high angle scattering, however detailed simulations show a much more rapid reduction (with number of shots) in the error associated with measurement of a difference in structure factor, due to pumping, than when using the conventional Monte Carlo method.

In conclusion, several new approaches to time-resolved XFEL diffraction have been presented. Of these, the convergent beam approach to reducing partiality in Bragg beams, the use of the mixing jet for time-resolved SAXS, and the use of the LCP jet in air for time-resolved pump–probe experiments may be implemented immediately. The development of split-and-delay schemes has undergone preliminary tests, while construction of the first attosecond hard X-ray laser may be some years away, in this rapidly evolving and exciting field of time-resolved atomic-resolution X-ray imaging.

Acknowledgements

I am grateful to Prof K. Schmidt and Prof U. Weierstall for many useful discussions. Supported by NSF STC award 1231306.

References

1 *Theory of X-ray diffraction in crystals*. W. H. Zachariasen. Dover 1967 Toronto.

2 T. Graber, S. Anderson, H. Brewer, Y. S. Chen, H. S. Cho, N. Dashdorj, R. W. Henning, I. Kosheleva, G. Macha, M. Meron, R. Pahl, Z. Ren, S. Ruan, F. Schotte, V. Srajer, P. J. Viccaro, F. Westferro, P. Anfinrud and K. Moffat, BioCARS: a synchrotron resource for time-resolved X-ray science, *J. Synchrotron Radiat.*, 2011, **18**(4), 658–670.

3 P. Emma, R. Akre, J. Arthur, R. Bionta, C. Bostedt, J. Bozek, A. Brachmann, P. Bucksbaum, R. Coffee, F.-J. Decker, Y. Ding, D. Dowell, S. Edstrom, A. Fisher, J. Frisch, S. Gilevich, J. Hastings, G. Hays, Ph. Hering, Z. Huang, R. Iverson, H. Loos, M. Messerschmidt, A. Miahnahri, S. Moeller, H.-D. Nuhn, G. Pile, D. Ratner, J. Rzepiela, D. Schultz, T. Smith, P. Stefan, H. Tompkins, J. Turner, J. Welch, W. White, J. Wu, G. Yocky and J. Galayda, First lasing and operation of an Ångstrom wavelength free-electron laser, *Nat. Photonics*, 2010, **4**(9), 641–647.

4 H. N. Chapman, P. Fromme, A. Barty, T. A. White, R. A. Kirian, A. Aquila, M. S. Hunter, J. Schulz, D. P. DePonte, U. Weierstall, R. B. Doak, F. R. N. C. Maia, A. V. Martin, I. Schlichting, L. Lomb, N. Coppola, R. L. Shoeman, S. W. Epp, R. Hartmann, D. Rolles, A. Rudenko, L. Foucar, N. Kimmel, G. Weidenspointner, P. Holl, M. Liang, M. Barthelmess, C. Caleman, S. Boutet, M. J. Bogan, J. Krzywinski, C. Bostedt, S. Bajt, L. Gumprecht, B. Rudek, B. Erk, C. Schmidt, A. Hömke, C. Reich, D. Pietschner, L. Strüder, G. Hauser, H. Gorke, J. Ullrich, S. Herrmann, G. Schaller, F. Schopper, H. Soltau, K. U. Kühnel, M. Messerschmidt, J. D. Bozek, S. P. Hau-Riege, M. Frank, C. Y. Hampton, R. G. Sierra, D. Starodub, G. J. Williams, J. Hajdu, N. Timneanu, M. M. Seibert, J. Andreasson, A. Rocker, O. Jönsson, M. Svenda, S. Stern, K. Nass, R. Andritschke, C. D. Schröter, F. Krasniqi, M. Bott, K. E. Schmidt, X. Wang, I. Grotjohann, J. M. Holton, T. R. M. Barends, R. Neutze, S. Marchesini, R. Fromme, S. Schorb, D. Rupp, M. Adolph, T. Gorkhover, I. Andersson, H. Hirsemann, G. Potdevin, H. Graafsma, B. Nilsson and J. C. H. Spence, Femtosecond X-ray protein nanocrystallography, *Nature*, 2011, **470**(7332), 73–77.

5 J. C. H. Spence, U. Weierstall and H. N. Chapman, X-ray lasers for structural and dynamic biology, *Rep. Prog. Phys.*, 2012, **75**, 102601.

6 Andrew Aquila, Mark S. Hunter, R. Bruce Doak, Richard A. Kirian, Petra Fromme, Thomas A. White, Jakob Andreasson, David Arnlund, Sa! a Bajt, Thomas R. M. Barends, Miriam Barthelmess, Michael J. Bogan, Christoph Bostedt, Hervé Bottin, John D. Bozek, Carl Caleman, Nicola Coppola, Jan Davidsson, Daniel P. DePonte, Veit Elser, Sascha W. Epp, Benjamin Erk, Holger Fleckenstein, Lutz Foucar, Matthias Frank, Raimund Fromme, Heinz Graafsma, Ingo Grotjohann, Lars Gumprecht, Janos Hajdu, Christina Y. Hampton, Andreas Hartmann, Robert Hartmann, Stefan Hau-Riege, Günter Hauser, Helmut Hirsemann, Peter Holl, James M. Holton, André Hömke, Linda Johansson, Nils Kimmel, Stephan Kassemeyer, Faton Krasniqi, Kai-Uwe Kühnel, Mengning Liang, Lukas Lomb, Erik Malmerberg, Stefano Marchesini, Andrew V. Martin, Filipe R. N. C. Maia, Marc Messerschmidt, Karol Nass, Christian Reich, Richard Neutze, Daniel Rolles, Benedikt Rudek, Artem Rudenko, Ilme Schlichting, Carlo Schmidt, Kevin E. Schmidt, Joachim Schulz, M. Marvin Seibert, Robert L. Shoeman, Raymond Sierra, Heike Soltau,

Dmitri Starodub, Francesco Stellato, Stephan Stern, Lothar Strüder, Nicusor Timneanu, Joachim Ullrich, Xiaoyu Wang, Garth J. Williams, Georg Weidenspointner, Uwe Weierstall, Cornelia Wunderer, Anton Barty, John C. H. Spence and Henry N. Chapman, Time-resolved protein nanocrystallography using an X-ray free-electron laser, *Optics Express*, 2012, **20**, 2706.

7 W. S. Graves, *et al.*, *Phys. Rev. Lett.*, 2012, **108**, 263904.

8 J. C. H. Spence, N. Zatsepin and C. Li, Coherent convergent-beam time-resolved X-ray diffraction, *Philos. Trans. R. Soc., B*, 2014, **369**, 20130325.

9 U. Weierstall, J. C. H. Spence and R. B. Doak, Injector for scattering measurements on fully solvated species, *Rev. Sci Instr.*, 2012, **83**, 035108.

10 D. Wang, J. C. H. Spence and U. Weierstall, A mixing jet for solution scattering at XFELs, *J. Synchrotron Radiat.*, 2014 Submitted.

11 R. Kirian, Structure determination through correlated fluctuations in X-ray scattering, *J. Phys. B*, 2012, **45**, 223001.

12 Uwe Weierstall, Daniel James, Dingjie Wang, Wei Liu, John C. H. Spence, R. Bruce Doak, Garrett Nelson, Petra Fromme, Raimund Fromme, Ingo Grotjohann, Christopher Kupitz, Nadia A. Zatsepin, Shibom Basu, Daniel Wacker, Chong Wang, Sébastien Boutet, Marc Messerschmidt, Garth J. Williams, Jason E. Koglin, M. Marvin Seibert, Cornelius Gati, Robert L. Shoeman, Anton Barty, Henry N. Chapman, Richard A. Kirian, Kenneth R. Beyerlein, Raymond C. Stevens, Dianfan Li, Syed T. A. Shah, Nicole Howe and Martin Caffrey, Lipidic cubic phase injector facilitates membrane protein serial femtosecond crystallography, *Vadim Cherezov Nature Communications*, 2014, **5**, 3309.

13 Richard A. Kirian, Thomas White, James Holton, Henry N. Chapman, Petra Fromme, Anton Barty, Lukas Lomb, Andrew Aquila, Filipe Maia, Andrew Martin, Raimund Fromme, Xiaoyu Wang, Mark Hunter, Kevin Schmidt and John C. H. Spence, Structure factor analysis of femtosecond microdiffraction patterns from protein nanocrystals, *Acta Cryst A*, 2011, **67**, 131–140.

14 H. N. Chapman, Phase-retrieval X-ray microscopy by Wigner-distribution deconvolution, *Ultramicroscopy*, 1996, **66**, 153–172.